

# A passive MEMS drug delivery pump for treatment of ocular diseases

Ronalee Lo · Po-Ying Li · Saloomeh Saati ·  
Rajat N. Agrawal · Mark S. Humayun · Ellis Meng

Published online: 25 April 2009  
© Springer Science + Business Media, LLC 2009

**Abstract** An implantable manually-actuated drug delivery device, consisting of a refillable drug reservoir, flexible cannula, check valve, and suture tabs, was investigated as a new approach for delivering pharmaceuticals to treat chronic ocular diseases. Devices are fabricated by molding and bonding three structured layers of polydimethylsiloxane. A 30 gauge non-coring needle was used to refill the reservoir; this size maximized the number of repeated refills while minimizing damage to the reservoir. The check valve cracking pressure was  $76 \pm 8.5$  mmHg (mean  $\pm$  SE,  $n=4$ ); the valve sustained  $> 2000$  mmHg of reverse pressure without leakage. Constant delivery at  $1.57 \pm 0.2$   $\mu$ L/sec and  $0.61 \pm 0.2$   $\mu$ L/sec (mean  $\pm$  SE,  $n=4$ ) under 500 mmHg and 250 mmHg of applied pressure, respectively, was obtained in benchtop experiments. The valve closing time constant was 10.2 s for 500 mmHg and 14.2 s for 250 mmHg. Assembled devices were successfully demonstrated in benchtop, *ex vivo*, and *in vivo* experiments.

**Keywords** Manual actuation · Drug pump · Polydimethylsiloxane · Ocular diseases

## 1 Introduction

### 1.1 Background

Drug delivery to ocular tissues is particularly difficult due to several factors including physiological barriers, space limitations in and surrounding the eye, and trauma to the eye associated with invasive therapies. However, for chronic eye diseases such as glaucoma, age-related macular degeneration (AMD), diabetic retinopathy, and retinitis pigmentosa, drug management is often the preferred first line of defense over surgical interventions to halt the progression leading to irreversible blindness (Geroski and Edelhauser 2000). These incurable diseases require lifelong treatment which currently includes one or more of the following methods: topically and orally administered medications, intraocular injections, and biodegradable drug implants.

Non-invasive drug delivery to the anterior and posterior segments of the eye is severely impeded by physiological barriers; eye drops and oral medications must permeate through the modified mucosal membrane of the cornea or the blood-retina barrier, respectively. For eye drops, it has been reported that only 5% of the dispensed drug may reach the anterior intraocular tissues through the cornea (Geroski and Edelhauser 2000). Furthermore, drug dilution due to lacrimation, tear drainage, and turnover limit the drug contact time with the cornea. Oral medications require larger doses to reach therapeutic levels due to presence of the blood-retina barrier. However, this may result in serious systemic side effects (Fraunfelder 1977, 1979, 1980, 1990;

---

R. Lo · E. Meng (✉)  
Department of Biomedical Engineering,  
Viterbi School of Engineering, University of Southern California,  
1042 Downey Way, DRB-140, Los Angeles, CA 90089-1111,  
USA  
e-mail: ellis.meng@usc.edu

P.-Y. Li · E. Meng  
Department of Electrical Engineering,  
Viterbi School of Engineering, University of Southern California,  
3651 Watt Way, VHE-602, Los Angeles, CA 90089-0241, USA

S. Saati · R. N. Agrawal · M. S. Humayun  
Department of Ophthalmology, Keck School of Medicine,  
University of Southern California,  
1450 San Pablo Street, DVRC 130, Los Angeles,  
CA 90033-1035, USA

Fraunfelder and Meyer 1984; Fraunfelder 2004; Fraunfelder and Fraunfelder 2004). While topical and oral medications are the simplest method of treatment, they rely on patient compliance and self-dosing.

Intraocular injections can directly bypass physiological barriers, however, the limited half-life of drugs in the vitreous cavity necessitates frequent injections (as many as 1–3 per week) for disease management (Lee et al. 2004). This method of treatment is suitable for treating acute bacterial infections, such as endophthalmitis, but is not suitable for chronic diseases such as AMD or cytomegalovirus (Mamalis et al. 2002). In addition, patient compliance is low. Frequent injections can induce trauma in ocular tissues such as cataracts, vitreous hemorrhage, and retinal detachment (Ambati et al. 2000).

Advanced ocular drug delivery systems that can provide both accurate and targeted dosing are urgently needed. Ideal drug delivery devices are biocompatible, result in minimal trauma and inflammation, provide localized delivery with minimal exposure to other tissues, provide sustained therapy (i.e. can be refilled), and have broad drug compatibility. Ocular drug delivery devices must also have a minimally-invasive footprint and not interfere with patient vision (Metrikin and Anand 1994).

There is limited real estate in the ocular orbit for an implantable device. The globe of the eye is positioned in a pyramidal shaped orbit. The medial wall of the orbit is only 7 mm from the globe (Smerdon 2000). This space is occupied by tissues such as extraocular muscles, orbital fat, and the Tenon's capsule (Jayaram and Calder 2004; Smerdon 2000). An ocular drug device that is placed in near proximity to the eye must fit within this space. Additionally, in order to prevent an infection pathway into the eye, the entire device should be encapsulated within the eye globe.

Delivery devices must function under a range of intraocular pressure (IOP) conditions. Reliable dose delivery under normal IOP conditions ( $15.5 \pm 2.6$  mmHg (mean  $\pm$  SD)) (Ritch et al. 1989), elevated conditions caused by diseases such as glaucoma (IOP > 22 mmHg), and transient conditions of fluctuating pressures due to outside influences such as patient sneezing, eye rubbing, or changes in altitude (e.g. flying) (Ritch et al. 1989; Wilensky 1999) is necessary.

### 1.2 Conventional ocular drug delivery devices

Existing ocular drug delivery devices can be categorized as (1) biodegradable or non-biodegradable, (2) atypical implantable systems, and (3) implantable pump systems. Biodegradable and non-biodegradable systems typically consist of a polymer matrix infused with drug or a reservoir containing drug, respectively. The drug is released as the

matrix dissolves or as the drug diffuses from the non-biodegradable reservoir. This form of drug delivery is dependent on drug load within the polymer (limited volume and cannot be refilled) and *in vivo* polymer degradation. Two commercially available devices, Vitrasert® and Retisert™, distributed by Bausch and Lomb utilize this method of delivery. The Vitrasert® and Retisert™ have a reported lifetime of 5–8 and 30 months, respectively. Atypical systems provide targeted delivery at a constant rate and minimize the drug volume required for treatment (Dash and Cudworth 1998). For example, hydrogel systems infused with drug swell via intake of biological fluids and release drug proportionally to the swelling rate. Existing ocular drug delivery devices fall into the first or last category. However, commercial sustained ocular drug delivery implants require repeated surgical interventions to implant and replace the device and also have similar side effects to those found in injection therapies.

Implantable pump systems provide control over delivery rate and volume when dispensing drug from an internal reservoir. Five types of implantable pump systems have been investigated: infusion pumps, peristaltic pumps, osmotic pumps, positive displacement pumps, and controlled release micropumps (Dash and Cudworth 1998). While implantable pump systems have been successfully executed for other drug delivery needs (e.g. insulin delivery, neurological compounds) (Grayson et al. 2004; Razzacki et al. 2004; Ziaie et al. 2004), due to ocular space limitations, currently available commercial devices are unsuitable for ocular drug delivery.

### 1.3 A MEMS ocular drug delivery device

MEMS (microelectromechanical systems) devices are routinely fabricated with micron-scale structures and can thus satisfy the spatial limitations on devices used in ocular drug delivery. Several single-use devices such as microneedles, micro/nano particles, and microreservoirs have been developed (Hilt and Peppas 2005). Microreservoirs provide the greatest delivery control of the three methods (Santini et al. 1999). Micro-well arrays are etched into a substrate, filled with drug, and then sealed using a thin membrane. Each well can be opened via electrochemical dissolution and thus release its contents to surrounding tissue. Different drugs can be loaded into the wells and discrete drug doses can be released on demand. However, this device cannot be refilled or reused which precludes its use in chronic eye disease management. Micropumps have been fabricated to provide controlled drug delivery via active pumping (Cao et al. 2001). Peristaltic pumps using a series of PZT actuators have been proposed and fabricated as a means of delivering drugs into the body. However, a large footprint (70 mm  $\times$  35 mm) is required to achieve 10  $\mu$ L/min flow. The pump

can be made smaller but at the cost of decreased pumping performance. Therefore, it would be difficult to achieve the flow rates necessary to deliver a wide range of dose volumes and regimens.

A novel refillable MEMS drug delivery device concept for treating chronic ocular diseases is presented. This device specifically addresses the shortcomings of conventional drug delivery methods. Using a MEMS approach, the device dimension limitations imposed by the ocular orbit can be met ( $< 2$  mm thick) and approved biocompatible materials can be used in device construction. Targeted drug delivery to the afflicted tissues that bypasses physiological barriers and a mechanism to prevent over-dosage or accidental dosage can be integrated into a single device. Broad drug compatibility of the delivery mechanism and reservoir enables greater utilization of novel pharmaceutical solutions and combination therapies. To improve patient compliance and reduce associated risks, the device must require only a single surgical intervention and be refillable. These features and added flexibility increase the potential for greater efficacy over current methods.

The prototype polymer MEMS delivery device consists of a refillable drug reservoir, transscleral cannula, check valve, support posts, and suture tabs. This is the first MEMS drug delivery device to feature a refillable reservoir (Lo et al. 2006; Lo et al. 2008). Surgical personnel have requested that the device have an internal volume of at least 200  $\mu\text{L}$  to minimize refills (no more than once per month). The target lifetime of this prototype is a minimum of 2 years. It is expected that future improvements to the device will further extend the lifetime of the device and ultimately reach the goal of a single device over the treatment period.

The device is surgically implanted with the reservoir placed underneath the conjunctiva, a membrane surrounding the eye. The cannula is inserted through the eye wall with the drug dispensing tip terminating in either the anterior or posterior segment depending on the site of treatment (Fig. 1(a), (b)). A specific dose of medication is dispensed from the device when the reservoir is mechanically actuated by the patient's finger. The increase in pressure within the reservoir forces the drug to travel down the enclosed microchannel within the transscleral cannula. A flow-regulating check valve (one-way valve) was incorporated near the tip of the cannula. The check valve responds to the pressure increase and opens, allowing drug to flow out of the device but prevents back flow of bodily fluids into the device. Support posts are contained within the microchannel and the reservoir to prevent stiction following the collapse of the device walls when the drug is depleted (Lo et al. 2008). Design consideration, fabrication process and characterization data of the prototype device is presented. Additionally, preliminary *in vitro*,

*ex vivo*, and *in vivo* experiments were conducted as a proof-of-concept for this first generation MEMS drug delivery device.

## 2 Design

The drug delivery device is formed from three layers of molded polydimethylsiloxane, or PDMS, (Sylgard 184, Dow Corning, Midland, MI) (Fig. 2). The bottom layer defines the base of the device, check valve seat, and suture tabs. The middle layer becomes one wall of the cannula and also contains the check valve orifice. The topmost layer completes the reservoir and defines the maximum drug volume that can be housed. The bottom and middle layer replicas were formed using silicon masters while the top layer was fabricated with a laser-machined acrylic mold.

The cannula and integrated check valve cross the eye wall via a scleral tunnel and enable targeted delivery to intraocular tissues either in the anterior or posterior segment. The cannula dimensions are determined by both ocular anatomy and surgical considerations. The cannula tip must not obscure the visual pathway (i.e. pupil) and the cannula should not come into contact with the cornea. These constraints limit the length of the cannula. The width and height of the cannula should be no more than 1 mm which corresponds to the maximum surgical incision size that the eye is able to self-seal. The cannula measures 10 mm  $\times$  1 mm  $\times$  1 mm. The internal dimensions of the cannula were chosen so as to minimize flow resistance (cross section of 0.5 mm  $\times$  0.1 mm).

The integrated check valve is a normally-closed, one-way valve. A post located at the tip of the cannula serves as the valve seat. The check valve is formed by aligning a 305  $\mu\text{m}$  diameter orifice over the valve seat at the end of the cannula. The valve opens when the applied pressure exceeds the cracking pressure of the valve. If the external pressure on the valve is higher than the internal pressure, the valve remains closed (Fig. 3). This prevents bodily fluids from entering the device and contaminating the drug. The cracking pressure of the check valve should be greater than IOP values that are found in the eye in order to prevent accidental dosing.

Square support posts (0.4 mm  $\times$  0.4 mm  $\times$  0.1 mm) to prevent cannula collapse and stiction, are located along the interior length of the cannula and in the reservoir (Fig. 2). The final support post located at the tip of the cannula serves as the valve seat for the check valve.

Four suture tabs provide surgeons a means for anchoring the device to the eye. Suture tabs are 2 mm in diameter and placed at each corner of the reservoir so that the anchoring sutures will not accidentally occlude or damage the cannula.

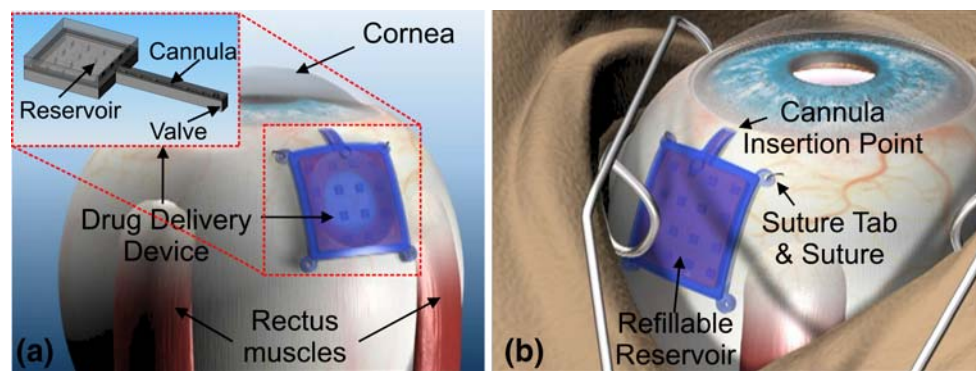


**Fig. 1** (a) Illustration of device placement. The size of the drug delivery device is limited by the available ocular space. Specifically, the device must fit between the rectus muscles and possess a low profile to avoid irritation (<2 mm). (b) Illustration of an implanted drug delivery device. The refillable reservoir is placed underneath the

conjunctiva (a thin layer of tissue covering the sclera) and sutured to the sclera (white portion of the eye). The cannula is inserted through the sclera into the eye. Inset: Overall device layout indicating the major components (*reservoir, cannula, valve*)

When the drug contained within the reservoir is depleted, the reservoir can be refilled with a non-coring needle. Device refill during *in vivo* studies was aided by the addition of a refill ring and rigid baseplate. The refill ring (stainless steel) allowed the surgeons to visually identify and target the refill location on the device. A hard baseplate made of polyetheretherketone (PEEK) controlled the penetration depth of the refill needle and prevented needle puncture through the entire device (Fig. 4(a), (b)).

### 3 Fabrication

The device layers were formed using soft lithography and master molds made of silicon or acrylic. The master molds for the bottom and middle layers were constructed from silicon wafers (Fig. 5(a), (b)). First, 4" silicon wafers were dehydration baked at 100°C for at least 30 min. The wafers were vapor coated with hexamethyldisilazane (HMDS)

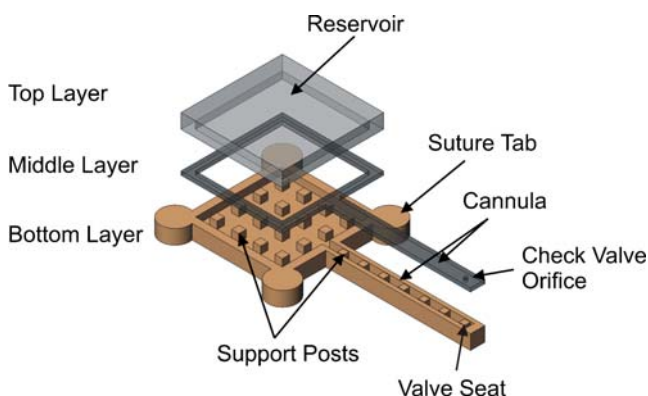


**Fig. 2** A three dimensional exploded view illustration of the three layers that form the device. The layers are individually fabricated using soft lithography techniques

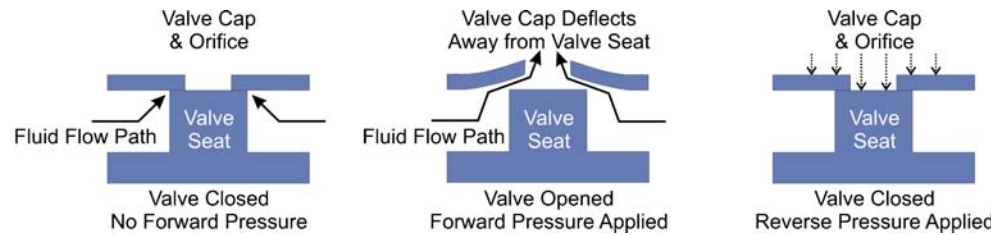
adhesion promoter. Photoresist (AZ 4620, AZ Electronic Materials, Branchburg, NJ) was spin coated at 2 krpm for 40 s (10 μm layer) (Fig. 6(a)). After exposure, native oxide was removed with a 10% hydrofluoric acid (HF) dip. 100 and 250 μm etch depths for the base and middle molds, respectively, were achieved using deep reactive ion etching (DRIE) (PlasmaTherm SLR-770B, Unaxis Corporation, St. Petersburg, FL) (Fig. 6(b)). Photoresist was removed using acetone, isopropyl alcohol (IPA), and deionized (DI) water. Then the wafers were cleaned using oxygen plasma (400 mTorr, 400 W, 4 min) (PEIIA, Technics Plasma, Kirchheim, Germany).

The silicon masters were cleaned using the RCA standard-clean-1 (SC-1) process (5:1:1 DI H<sub>2</sub>O:H<sub>2</sub>O<sub>2</sub>:NH<sub>4</sub>OH) to remove any organic compounds. The masters were then coated with approximately 5 μm of vapor deposited Parylene C (Specialty Coating Systems, Inc., Indianapolis, IN) (Fig. 6(c)). The Parylene C film served as a release layer to facilitate the removal of the PDMS replica from the mold.

PDMS was mixed (10:1 base to curing agent ratio; AR-250 Hybrid Mixer, Thinky Corp., Tokyo, Japan), poured, and spread over the silicon master (Fig. 6(d)). The depth of features on the master defined the height of the molded structures thus excess PDMS was removed from the master. The PDMS was degassed in a vacuum oven (Model VO914A, Lindberg/Blue, Asheville, NC) and cured (90°C for 1 h). The molded sheet of PDMS was gently separated from the silicon master (Fig. 6(e)). Individual device layers were dissected from the PDMS sheet using a fine-tipped blade (Fig. 6(f)).

The mold for the top layer was fabricated by using a machined Plexiglas mold. Plexiglas sheets (1.59 mm thick) were cut using a laser machining center (Mini/Helix 8000, Epilog, Golden, CO) into squares corresponding to the desired interior reservoir volume. The Plexiglas squares

**Fig. 3** Illustration of check valve operation under forward and reverse pressure conditions



were glued (Loctite Professional Epoxy, Henkel Consumer Adhesives, Inc., Avon, OH) to a glass microscope slide (Gold Seal Micro Slides (glass type 0211), Erie Scientific Company, Portsmouth, NH) and placed in a Petri dish. PDMS (10:1 base to curing agent) was mixed and poured over the mold. However, unlike the silicon masters, excess PDMS (extending approximately 1 mm above the surface of the mold) was poured over the mold in order to create the top wall of the reservoir. After degassing, PDMS was partially-cured (90 °C for 30 min). PDMS was separated from the mold and then individual reservoirs were dissected. Reservoirs having volumes of 39.7  $\mu\text{L}$  (5 mm  $\times$  5 mm  $\times$  1.59 mm) and 57.2  $\mu\text{L}$  (6 mm  $\times$  6 mm  $\times$  1.59 mm) were fabricated.

The check valve orifice was formed by coring the PDMS sheet forming middle layer with a 30 gauge (305  $\mu\text{m}$  outer diameter) coring needle (91030, Hamilton Company, Reno, NV). When the needle was inserted, it cut through the sheet forming a cylindrical hole. The coring site was aligned over the check valve seat located at the end of the cannula (Fig. 7). In order to ensure that the cylindrical hole and valve seat were aligned, a small post indicating the hole location was incorporated into the silicon master.

The bottom and middle layers were cleaned in 0.01% hydrochloric acid (HCl) and then rinsed in DI water. The bonding surfaces were treated by exposure to oxygen plasma (DP80M RIE, Plasma Technology LTD, United Kingdom); 100 W and 100 mTorr for 45 s. Oxygen plasma treatment enables the formation of irreversible bonds between separate PDMS pieces (McDonald et al. 2000). Ethanol was used to extend the lifetime of the oxygen plasma modified surface and to lubricate the layers during

alignment (McDonald and Whitesides 2002). After the bottom and middle layers are joined, the half-cured top layer was placed on the assembly. The device was left at room temperature for 24 h to allow the top layer to completely cure.

The final structure was mechanically-reinforced by applying a thin PDMS layer around the perimeter of the device (Unger et al. 2000; Wu et al. 2005). The reinforcing layer was formed by pouring PDMS prepolymer (10:1 base to curing agent ratio) around the device. The device was placed at an incline in a Petri dish to prevent PDMS prepolymer from covering the check valve. The reinforcing layer was cured at 90 °C for 1 h. Excess PDMS material was removed from the device. The reinforcing layer was deemed necessary to achieve a more robust device that could withstand surgical manipulation during the *ex vivo* and *in vivo* studies.

## 4 Experimental methods

### 4.1 PDMS-to-PDMS bonding

Qualitative comparison of oxygen plasma and chemical treatment methods to bond PDMS in both benchtop prototypes and surgical models were conducted. Bonding strength was qualitatively assessed by observing the fracture resistance of the bond to an applied shear force. PDMS sample coupons were prepared (20 mm  $\times$  10 mm) and cleaned using in a 0.01% HCl solution. Pairs of coupons were exposed to oxygen plasma or wet chemical treatment (0.012 M HCl) and assembled such that half of each coupon overlapped the other coupon. Force was applied by pulling on the non-overlapping sections of the coupons.

Oxygen plasma treatment of PDMS results in a hydrophilic surface due to the formation of silanol groups (Si-OH). When two treated surfaces are joined, irreversible covalent bonds (Si-O-Si) form. The number of silanol groups formed depends on conditions of the plasma treatment (duration, power, and pressure). Polar solutions such as water and ethanol can extend the reactive time of the silanol groups and slows the return of the surface to its original hydrophobic state (McDonald et al. 2000). Baking the bonded sample can also increase the strength of the bond (McDonald and Whitesides 2002). Oxygen plasma

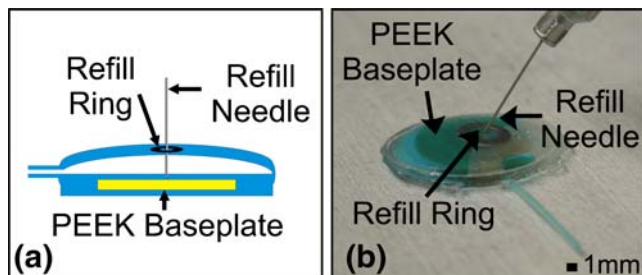


**Fig. 4** (a) Illustration of side view of hollow surgical sham. (b) Verification of benchtop refill of a hollow surgical sham through the refill ring using a 30G needle

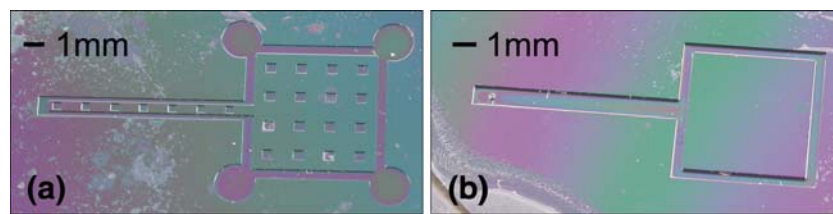


**Fig. 5** Image of a silicon mold used to create the (a) bottom and (b) middle layers for the drug delivery device. The silicon masters were coated in Parylene C to facilitate mold release of the PDMS layer from the master

power, pressure, and duration were examined to determine the optimal conditions for maximum bonding strength. Water and ethanol were used to facilitate alignment prior to bonding. Baking time and temperature were also examined.

Chemical treatment of PDMS to promote bonding was also evaluated. Samples of PDMS were immersed in 0.012 M HCl. Samples were removed and rinsed with ethanol, blown dry, and assembled. Baking temperature, baking time, and bond compression during baking were examined.

#### 4.2 Check valve characterization

Check valve performance was characterized using a custom laser-machined Plexiglas test jig (Fig. 8(a)). The bottom and middle layers of the device were aligned and placed in the jig. A pressurized water source was connected to the input of the jig and a calibrated pipette (100  $\mu$ L, Clay Adams, Parsippany, NJ) to the output (Fig. 8(b)). The pipette was primed by pre-filling it with water. A small air bubble was introduced at the input of the pipette. As small increments of pressurized water were applied to the check valve, the bubble position was monitored. After each pressure increase, the system was held at a constant pressure to allow the system to equilibrate (3 min). The cracking pressure of the check valve was recorded and the flow rate at greater applied pressures was determined by measuring

the distance an air bubble moved along the calibrated 100  $\mu$ L pipette over a 3 minute time interval.

The reverse pressure performance was tested by connecting the pressurized water source to the output of the jig and the calibrated pipette to the input. An air bubble within the pipette was monitored to determine if any leakage occurred during the application of reverse pressure on the device.

Check valve dosing while varying the applied pressure and the duration of the pressure was also measured. An electronically-controlled solenoid valve (LHDA0533115H, The Lee Company, Westbrook, CT) was used to vary the duration of the applied pressure to simulate a patient's finger. A square wave control signal with a 50% duty cycle and frequencies ranging from 50 mHz to 500 mHz was used to control a pressurized water source. In the "on" state, the solenoid permits pressurized water to be passed onto the jig. The volume of fluid exiting the valve is measured by noting the distance an air bubble traveled in a calibrated pipette (100  $\mu$ L) over the "on" and "off" portion of the wave. The closing time constant for the valve was determined by measuring the elapsed time between removing the pressure from the valve and when the accumulated volume exiting the valve reached 63.2% of the final volume.

#### 4.3 Refill needle and refillability

Device lifetime is closely linked to the ability to refill the reservoir with a syringe needle and the mechanical integrity

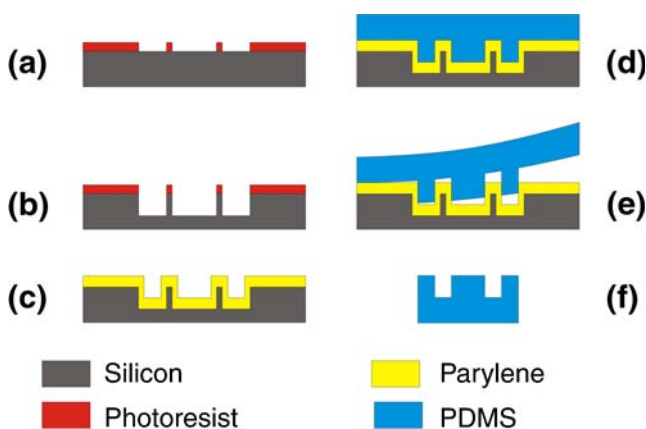


**Fig. 6** Soft-lithography fabrication process used to fabricate the bottom and middle layers of the device

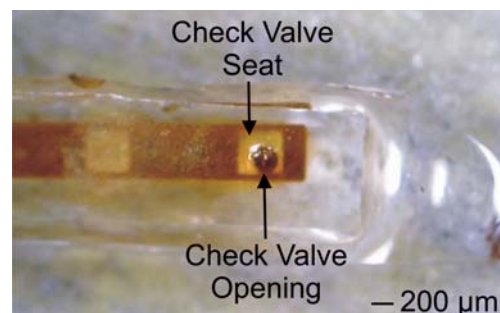
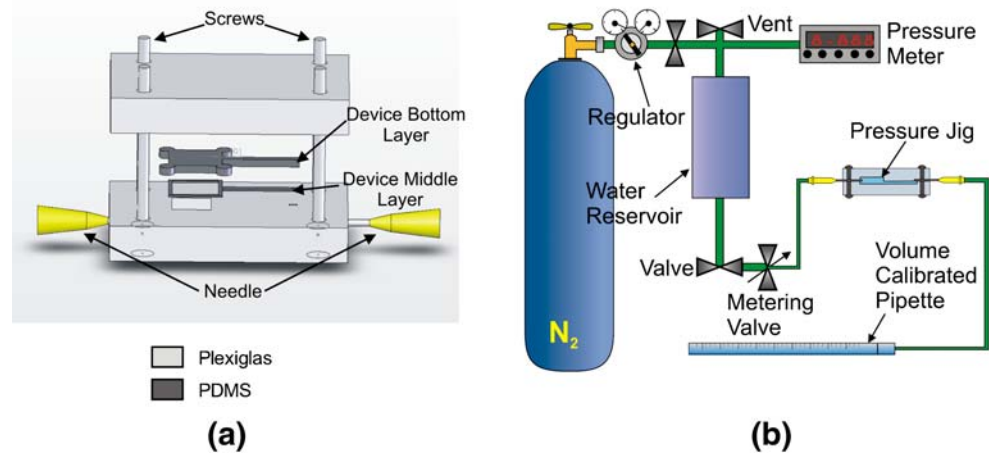


**Fig. 7** Top view of the check valve located at the tip of the cannula. The cannula was filled with fluorescein to facilitate visualization of its individual components

**Fig. 8** (a) Laser-machined jig used to characterize check valve performance. The bottom and middle layers were aligned and clamped within the jig. (b) Pressurized system used in conjunction with the check valve testing jig to evaluate valve performance. A calibrated pipette was used to determine flow rate values



of the punctured material. Therefore, the maximum number of achievable refills must be determined.

Commercially available needles can be used to refill the device. A 30 gauge (305  $\mu\text{m}$  in outer diameter) needle was used to refill the device. This size was selected as a trade-off between maintaining a small outer diameter needle to maximize material lifetime and ease of handling (e.g. stiff enough to puncture device without needle bending). The needle must pierce the conjunctiva and reservoir wall in order to replenish the reservoir contents. This needle size also permits resealing of the puncture in the conjunctiva thus avoiding the need for sutures.

Two types of 30 gauge needles, coring and non-coring, were investigated to determine the most suitable needle profile. The needle must be able to puncture the PDMS reservoir but cause minimal damage to the material after removal. Both types of needles were inserted through PDMS slabs. The needle tracks through the PDMS and at the insertion sites were examined.

PDMS membranes (250  $\mu\text{m}$  and 670  $\mu\text{m}$  thick) were evaluated for mechanical integrity by testing for leaks after repeated punctures (or refill events). PDMS sheets were obtained by spreading a thin layer of PDMS (10:1 base to curing agent ratio) on a glass substrate and curing at 90  $^{\circ}\text{C}$  for 20 min. 12.7 mm  $\times$  12.7 mm square membranes were cut from the sheet. Each membrane was mounted in a custom laser-machined Plexiglas jig containing a small hole to align repeated needle punctures in the same location (8, 12, and 24 trials) (Fig. 9(a)). This represents the worst-case scenario in which each subsequent puncture potentially enlarges the puncture hole and increases the likelihood of leakage. After puncturing, the membrane was transferred to the second jig in which the puncture site was aligned between two reservoirs (Fig. 9(b)). The input of the jig was attached to a pressurized water system and the output was connected to a calibrated pipette (50  $\mu\text{L}$ , Clay Adams, Parsippany, NJ) (Fig. 9(c)). Pressurized water was applied in increments and water leakage, if any, was monitored by tracking the position

of small bubble in the water-filled calibrated pipette. The leakage rate was determined by measuring the velocity at which a bubble moved through a pipette. The burst pressure of unpunctured membranes was also measured.

#### 4.4 Surgical studies

Several surgical methods to attach the device to the sclera and introduce the cannula into the anterior chamber of the eye were investigated. Enucleated porcine eyes were used to conduct the initial *ex vivo* studies. The position, size, and shape of the suture tabs were optimized to secure the device to the sclera. Surgical handling resulted in separation of the device layers; more robust bonding techniques were investigated to produce a surgically robust device. Surgical techniques were developed to position the cannula in the anterior chamber of the eye; this location is desirable for the treatment of anterior chamber diseases such as glaucoma. Device functionality was tested following surgical implantation. Dyed deionized (DI) water was dispensed by introducing mechanical pressure on the reservoir with forceps. The cannula insertion site was carefully monitored for leakage. After emptying the reservoir, refilling was performed. Dispensing and refilling were repeated in several trials.

*In vivo* verification of dispensing was also conducted in male Dutch Belted pigmented rabbits. The device was filled with phenylephrine, a pupil dilating agent. Phenylephrine was dispensed and temporal changes in pupil size were noted.

## 5 Results and discussion

### 5.1 Bonding

Bonds created following oxygen plasma were found to be more reliable than those created following wet chemical treatment. Optimized oxygen plasma conditions were determined to be 100 W, 100 mTorr, and 45 s. Once the

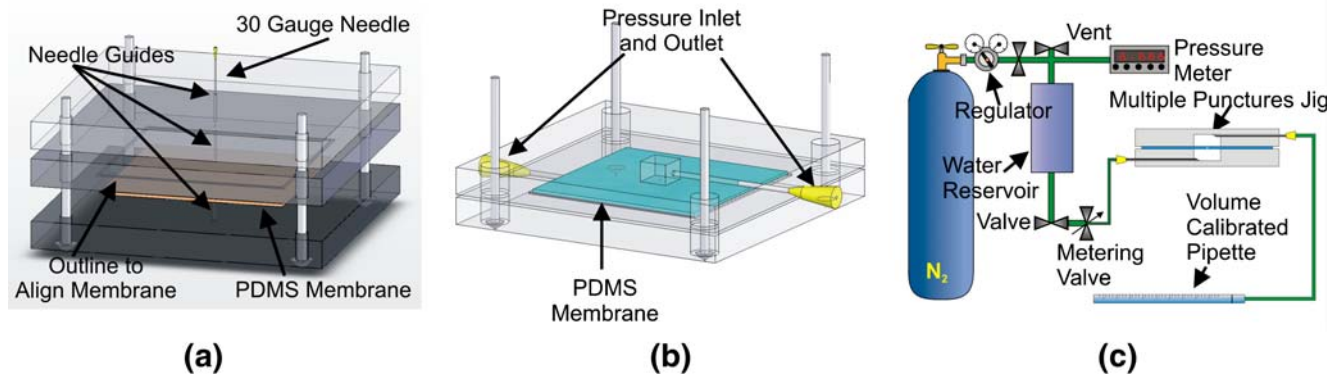


**Fig. 9** (a) Laser-machined jig used to align multiple needle punctures through the same point in a silicone membrane. This jig ensured that all of the punctures pierced the same location; this is the worst-case scenario

for refill and potential leakage failure through the refill hole. (b) Laser-machined jig to pressurize the punctured membrane. (c) Pressure system used to evaluate leakage through the needle puncture track

surfaces of the layers were treated, the layers were aligned with the aid of a polar liquid (e.g. ethanol or water). The entire assembly was then baked at 100°C for 45 min in order to complete the bonding process (Duffy et al. 1998).

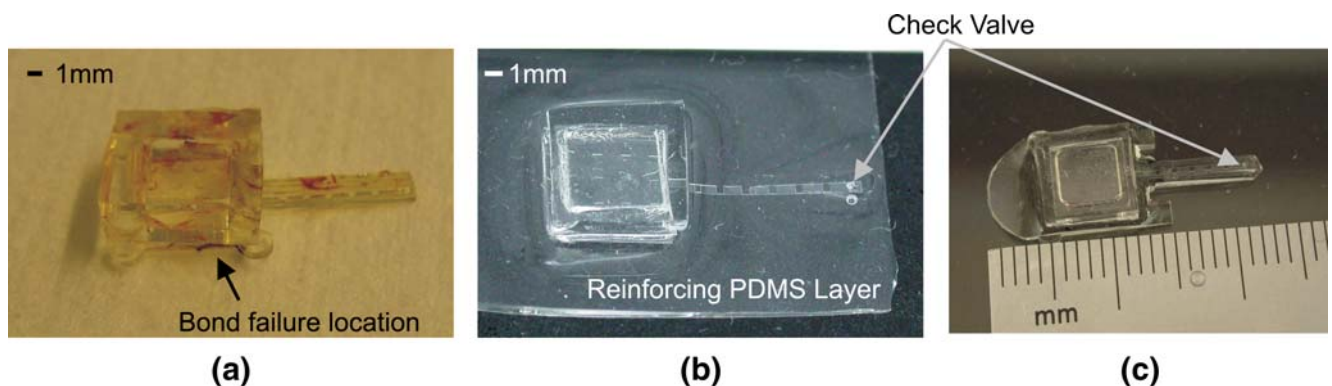
However, the bond strength was insufficient to survive handling encountered during device implantation (Fig. 10(a)). For example, the surgical procedure required bending the cannula back on itself (180° bend) to insert it into an incision in the eye. The two layers forming the cannula delaminated during this procedure. Thus, the bonds were strengthened using a reinforcing layer of PDMS around the periphery of the device (Fig. 10(b)). The reinforcing layer was trimmed to remove excess material and to create suture tabs (Fig. 10(c)). The reinforced device was able to survive extensive surgical handling and did not fail during benchtop testing or implantation.

## 5.2 Check valve characterization

The integrated check valve was characterized to determine the cracking pressure, forward flow rates, and reverse

pressure performance. A representative cracking pressure is  $76 \pm 8.5$  mmHg (mean  $\pm$  SE,  $n=4$ ) ( $10.2 \pm 1.1$  kPa). The cracking pressure was highly dependent on valve alignment as well as variations introduced by the testing jig, therefore, the cracking pressures of several valves were found to vary slightly. However, all measured cracking pressures were much higher than normal IOPs found within the eye ( $15.5 \pm 2.6$  mmHg (mean  $\pm$  SD)) (Ritch et al. 1989). This condition is necessary to prevent the device from accidentally dispensing due to normal activities that may impose temporary pressure on the device, such as sneezing or rubbing the eyes. The valve design can be modified to target operation within a specified pressure range if necessary. Flow rate increased when the pressure on the system was increased. The range of actuation pressures was determined by the range of interest for ocular dispensation as well as the limits of the pressure testing system. Additionally, the check valve was able to withstand at least 2000 mmHg (266.6 kPa) of reverse pressure without valve leakage or failure (Fig. 11).

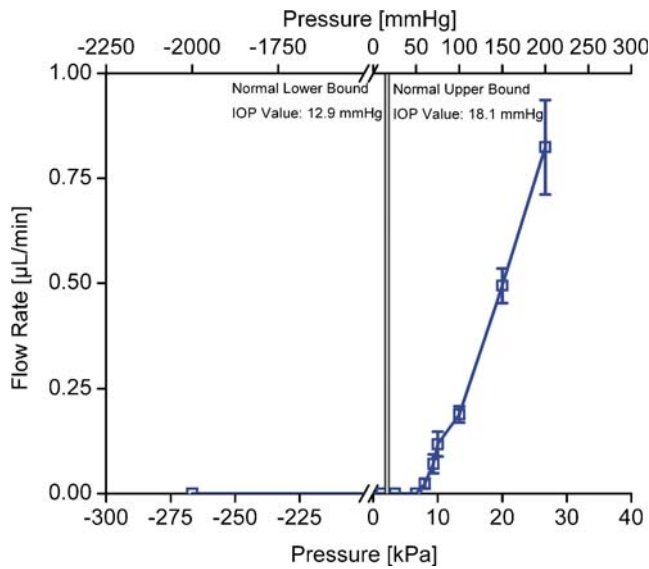
Dosed volume was measured for two different applied pressures 250 mmHg (33.33 kPa) and 500 mmHg



**Fig. 10** (a) Implanted *in vivo* device (plasma bonded) with band failure location identified. (b) Reinforcing layer added to bonded device in order to provide more mechanical robustness. (c) Excess

silicone was removed from the device to create the desired device outline, ruler divisions measure 1 mm

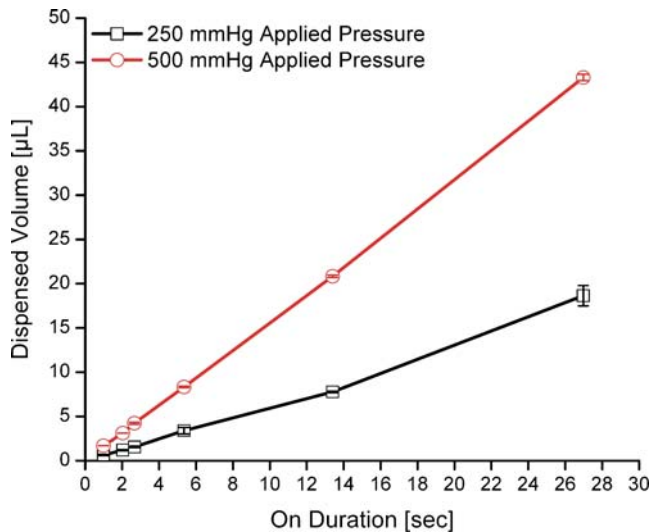




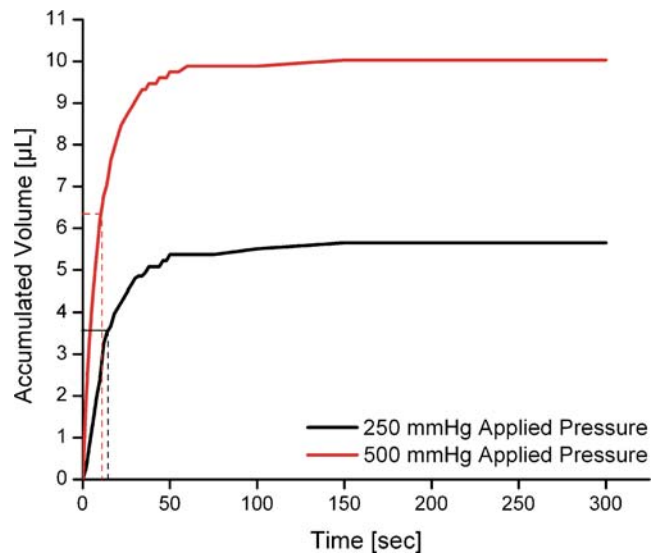
**Fig. 11** Check valve characterization curve (diode curve). The valve opened at a cracking pressure of  $76 \pm 8.5$  mmHg (mean  $\pm$  SE,  $n=4$ ) ( $10.2 \pm 1.1$  kPa) and was able to withstand reverse pressures in excess of 2000 mmHg (266.6 kPa) without leaking or failing. Normal IOP values are indicated in the shaded region

(66.66 kPa) controlled using a 50% duty cycle square wave control signal in the frequency range 18.5 mHz to 500 mHz (53 to 2 sec periods). Dosed volume and pressure duration were found to be linearly proportional for both applied pressures, resulting in a consistent flow rate independent of the dosing period (Fig. 12). The steady state flow rates were  $1.57 \pm 0.2 \mu\text{L}/\text{sec}$  and  $0.61 \pm 0.2 \mu\text{L}/\text{sec}$  (mean  $\pm$  SE,  $n=4$ ) at 500 mmHg and 250 mmHg, respectively.

Due to the finite closing time of the valve, flow was observed after removal of the pressure source. The time



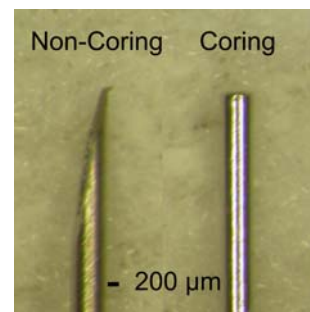
**Fig. 12** Check valve control of dosing under 250 mmHg and 500 mmHg of applied pressure. Duration of applied pressure was varied using a solenoid valve controlled using 50% duty cycle square waves



**Fig. 13** A representative graph depicting the volume dispensed after the applied pressure (250 mmHg and 500 mmHg) is removed from the valve. The dashed lines indicate when the accumulated volume reached 62.3% of the final value, the time at which this point occurred was defined as the closing time constant for the valve

constant associated with valve closing was found to be 10.2 s for 500 mmHg and 14.2 s for 250 mmHg (Fig. 13). Dispensed volume and closing time calculations could not be measured in real-time, therefore these data were extracted from video footage of the air bubble moving through the calibrated pipette. Dosed volume was calculated using initial and final bubble positions in the pipette and the applied pressure duration was calculated from the time stamps in the video. The closing time constant was calculated by noting the bubble location starting from when pressure was removed and at specific time intervals until the bubble movement stopped. The closing time constant was calculated by determining the time at which the accumulated volume reached 62.3% of the final value. The volume dispensed over the duration of closing time is  $3.5 \mu\text{L}$  and  $6.3 \mu\text{L}$  for 250 mmHg and 500 mmHg, respectively. The long closing time constant can significantly increase the dosage amount, especially for very small dosages. Additionally, the valve does not prevent accidental dosing due to transient fluctuations in intraocular pressures

**Fig. 14** Optical image of coring and non-coring 30 gauge (O.D. 305  $\mu\text{m}$ ) needles



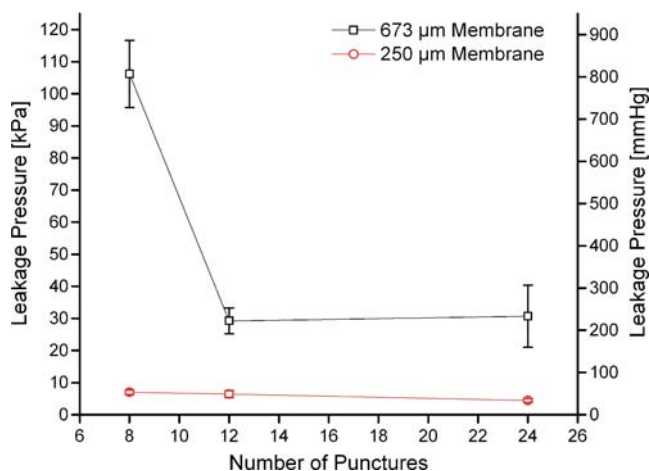


**Fig. 15** Leakage pressure after 8, 12, and 24 punctures using a 30 gauge non-coring needle through 673  $\mu\text{m}$  and 250  $\mu\text{m}$  thick silicone membranes (mean  $\pm$  SE,  $n=4$ )

(e.g. sneezing, flying). Therefore, improvements in response time and overpressure protection will be incorporated in future drug delivery device prototypes.

### 5.3 Refill needle

Optical microscope images of 30 gauge coring and non-coring needles were taken to examine the needle tip and needle shaft. The coring needle has a blunt tip with a circular cutting edge. The non-coring needle has a beveled tip which tapers to a point (Fig. 14).

Both needles were pushed into and withdrawn from a sample piece of PDMS. The resulting needle puncture entrance and needle track were imaged using an optical microscope. A coring needle removed material as it was pushed through a sample. When the needle was removed, a cylindrical hole was formed through the PDMS slab. The non-coring needle displaces material as it moves through

the sample and creates a small tear. The material relaxes when the needle is removed and seals the tear. A non-coring needle was selected for refilling and maximizing device lifetime (Lo et al. 2008).

### 5.4 Refillability

The maximum pressure a repeatedly punctured membrane can withstand without leaking decreases as the number of punctures increases. The burst pressure for the 673  $\mu\text{m}$  membrane (525.75 kPa, 3943.5 mmHg) was 5 times larger than the leakage pressure for 8 punctures (106.2 kPa, 796.4 mmHg), while the burst pressure for the 250  $\mu\text{m}$  membrane (393.5 kPa, 2951.1 mmHg) was 56 times larger than the 8 puncture leakage pressure (6.98 kPa, 52.4 mmHg). As expected, the thicker membrane was able to better tolerate the damage from multiple punctures. For all of the repeated puncture tests, the leakage pressure for both membranes decreased with increasing number of punctures. The thicker membrane was able to support higher pressures. The leakage pressure for both membranes approached a constant value for higher puncture numbers (Fig. 15). This may be attributed to nominal or lack of additional damage to the needle track for each subsequent needle puncture.

Two needle puncture arrangements were examined to determine the impact of spatial arrangement on membrane strength. For the case where all punctures were created at the same position on a 250  $\mu\text{m}$  thick membrane, the resulting leakage pressure after 8 punctures was  $6.98 \pm 0.73$  kPa (mean  $\pm$  SE,  $n=4$ ) ( $52.36 \pm 5.48$  mmHg). The second case involved puncturing a 250  $\mu\text{m}$  membrane punctured 8 times in random locations in a 5 mm  $\times$  5 mm square area and resulted in a leakage pressure of  $8.14 \pm 0.07$  kPa (mean  $\pm$  SE,  $n=3$ ) ( $61.02 \pm 0.52$  mmHg). Aligning the needle punctures in exactly the same position lowered

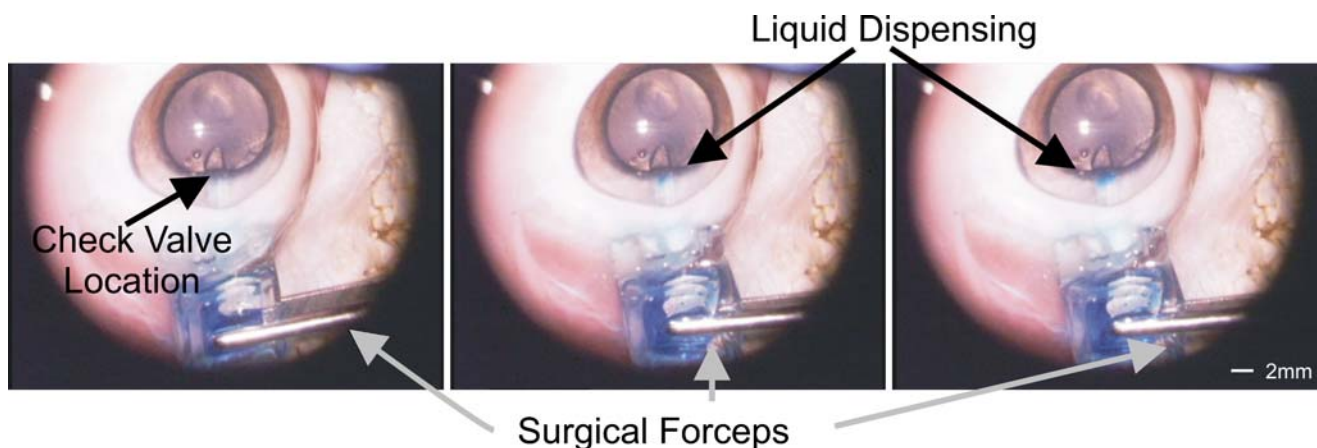


**Fig. 16** Demonstration of successful *ex vivo* dispensing in an enucleated porcine eye. The cannula was inserted into the anterior chamber via a scleral tunnel. Surgical forceps were used to depress the reservoir in order to dispense dyed liquid from the device reservoir into the eye

**Table 1** Partial list of fabricated surgical shams with major dimensions

Sham	v2_small	v3_1	v3_2	v4_1	v5_1	v6_1
Solid/ Hollow	Solid	Solid	Hollow	Hollow	Hollow	Hollow
Material	PDMS/ MDX4-4210	PDMS/ MDX4-4210	PDMS/ MDX4-4210	PDMS/ MDX4-4210	MDX-4210	MDX4-4210
Major Axis Length [mm]	15.9	16.9	16.9	16.9	9.8	9.8
Minor Axis Length [mm]	12	13	13	13	7.7	7.7
Thickness [mm]	2.00	2.00	1.9	1.9	1.7	1.7
Internal Volume [ $\mu$ L]	N/A	N/A	126.1	126.1	42.9	42.9
Refill Ring ID [mm]	2.9	2.9	2.9	2.9	2.0	2.0
Refill Ring OD [mm]	5.31	5.31	5.31	5.31	4.76	4.76
Baseplate Size [mm]	N/A	N/A	N/A	Diameter:11.7	Diameter: 6.5	Oval 9.845 x 7.7

the leakage pressure of the membrane. This was likely associated with an increase in puncture size as a result of repeated needle insertions. For the randomly located puncture case, each puncture was associated with only one insertion event and thus the needle track size was minimized.

The device was successfully refilled in benchtop experiments using a standard 30 gauge non-coring needle attached to a syringe. In between each refill event, the reservoir was manually depressed to dispense the dyed DI water through the cannula and check valve.

### 5.5 Surgical studies

Dispensation and refill were also tested *ex vivo*. The device placement and cannula insertion were demonstrated using enucleated porcine eyes. Surgical studies determined that only two sutures, located on the front corners of the device, were sufficient to secure the device to the sclera. The cannula of the sutured device was inserted into the anterior chamber via a scleral tunnel. Dyed DI water could be seen entering the eye when the reservoir was manually depressed with blunt surgical forceps (Fig. 16). Once the device was depleted, the reservoir was refilled using a 30 gauge non-coring needle. Device dispensing and refill were successfully executed multiple times during the study. The limited space in the anterior chamber imposes a thickness con-

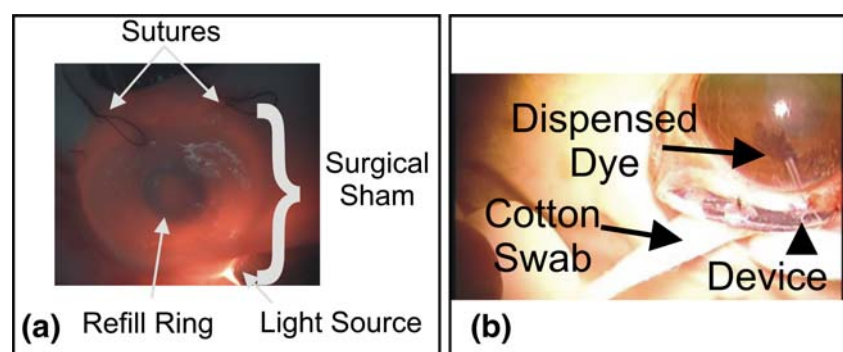
straint on the cannula and on valve operation. For example, valve operation was obstructed when in contact with the cornea. Additionally, corneal damage may occur from prolonged device contact as was observed in surgical studies performed with sham devices.

*In vivo* delivery of phenylephrine resulted in measurable physiological responses. Vertical and horizontal pupil lengths were 6.5 mm and 6 mm, respectively, prior to phenylephrine dispensation. After dispensation, vertical and horizontal lengths increased to 8 mm and 7 mm, respectively (Lo et al. 2008).

A series of surgical shams (solid and hollow) were fabricated to provide models to improve the surgical protocol and allow surgeons to practice device refill (Table 1). Each version of the sham included design improvements to aid surgical implantation. These shams had a more compatible morphology than the rectangular first generation device and could be used for chronic implant studies. Surgical shams were also used to rapidly prototype and test device components and their placement on the device (e.g. a metal ring to designate a target refill location. Transillumination of the eye enhances the visibility of the refill ring through the ocular tissue (e.g. conjunctiva) (Fig. 17(a)).

The refill ring may also be located using ultrasound or optical coherence tomography (OCT) if the equipment is

**Fig. 17** (a) Transilluminated device to help visualize the location of the surgical sham and refill ring. (b) Demonstration of successful *In vivo* delivery of dyed liquid from the surgical sham into the anterior chamber of the eye



available in out-patient offices. *In vivo* tests of the surgical sham also verified device functionality using a rounded dome-shaped reservoir instead of a square reservoir (Fig. 17(b)).

A valveless cannula (I.D. 305  $\mu\text{m}$ , O.D. 610  $\mu\text{m}$ ), constructed using commercially available silicone tubing (60985-700, VWR, West Chester, PA), was incorporated into the surgical shams. Chronic refill and dispensing studies (>6 months) of the hollow surgical shams demonstrated no blockage or obstruction of the cannula due to biofouling. Chronic studies with valved devices are planned.

## 6 Conclusion

A manually-actuated drug delivery device that can be utilized as a method of treatment for chronic ocular diseases has been demonstrated. Device components such as the refillable reservoir and check valve were characterized. The maximum internal pressure the reservoir can withstand, after multiple punctures using a 30 gauge non-coring needle, was determined to initially decrease with additional punctures, but showed no significant decrease after 12 punctures. The check valve diode curve was measured to determine cracking pressure and pressure versus flow rate values. Check valve regulated delivery and closing time constants were also determined. The device was tested in benchtop and *ex vivo* experiments including device dispensing and refill. *In vivo* experiments demonstrated successful drug delivery resulting in the corresponding physiological response. This ocular drug delivery system is broadly compatible with existing ophthalmic drugs and will be further investigated for chronic treatment of ocular diseases.

**Acknowledgments** This work was funded in part by the Engineering Research Centers Program of the NSF (EEC-0310723), NIH (1R21EY018490-01), NIH core grant (EY03040), an unrestricted grant by Research to Prevent Blindness, and Bausch and Lomb. The authors would like to thank Mr. Trevor Roper and Mr. Merrill Roragen for fabrication assistance, Dr. Yu-Chong Tai for providing access to the Caltech Micromachining Laboratory Cleanroom, Ms. Lilian Tran for conducting PDMS bonding experiments, Mr. Kenrick Kuwahara for his contributions to optimizing the assembly of the drug delivery device, Mr. Tun Min Soe for artistic illustrations of the device in the eye, and Ms. Mei Li Nickles for creating the SolidWorks images of the test jigs.

## References

- J. Ambati, E.S. Gragoudas, J.W. Miller, T.T. You, K. Miyamoto, F.C. Delori, A.P. Adamis, *Invest. Ophthalmol. Vis. Sci.* **41**, 5 (2000)
- L. Cao, S. Mantell, D. Polla, *Sens. Actuators A Phys* **94**, 1–2 (2001). doi:10.1016/S0924-4247(01)00680-X
- A.K. Dash, G.C. Cudworth 2nd, *J. Pharmacol. Toxicol. Methods* **40**, 1 (1998). doi:10.1016/S1056-8719(98)00027-6
- D.C. Duffy, J.C. McDonald, O.J.A. Schueller, G.M. Whitesides, *Anal. Chem.* **70**, 23 (1998). doi:10.1021/ac980656z
- F.T. Fraunfelder, *JAMA* **237**, 5 (1977). doi:10.1001/jama.237.5.446b
- F.T. Fraunfelder, *Ophthalmology* **86**, 1 (1979)
- F.T. Fraunfelder, *Ophthalmology* **87**, 2 (1980)
- F.T. Fraunfelder, *J. Am. Ophthalmol* **110**, 4 (1990)
- F.T. Fraunfelder, S.M. Meyer, *J. Aust. Ophthalmol* **12**, 2 (1984)
- F.W. Fraunfelder, *Insight* **29**, 2 (2004)
- F.W. Fraunfelder, F.T. Fraunfelder, *Ophthalmology* **111**, 7 (2004)
- D.H. Geroski, H.F. Edelhauser, *Invest. Ophthalmol. Vis. Sci.* **41**, 5 (2000)
- A.C.R. Grayson, R.S. Shawgo, Y.W. Li, M.J. Cima, *Adv. Drug Deliv. Rev.* **56**, 2 (2004)
- J.Z. Hilt, N.A. Peppas, *Int. J. Pharm* **306**, 1–2 (2005). doi:10.1016/j.ijpharm.2005.09.022
- H. Jayaram, I. Calder, *Anaesth. Intensive Care Med.* **5**, 9 (2004). doi:10.1383/anes.5.9.300.49895
- S.S. Lee, P. Yuan, M.R. Robinson, *Encyclopedia of Biomaterials and Biomedical Engineering*, (2004)
- R. Lo, K. Kuwahara, P.Y. Li, R. Agrawal, M.S. Humayun, E. Meng, (Okinawa, Japan, 2006), pp. 4
- R. Lo, P.Y. Li, S. Saati, R. Agrawal, M.S. Humayun, E. Meng, *Lab Chip* **8**, 7 (2008)
- N. Mamalis, L. Kearsley, E. Brinton, *Curr. Opin. Ophthalmol.* **13**, 1 (2002). doi:10.1097/00055735-200202000-00004
- J.C. McDonald, D.C. Duffy, J.R. Anderson, D.T. Chiu, H.K. Wu, O.J.A. Schueller, G.M. Whitesides, *Electrophoresis* **21**, 1 (2000). doi:10.1002/(SICI)1522-2683(20000101)21:1<27::AID-ELPS27>3.0.CO;2-C
- J.C. McDonald, G.M. Whitesides, *Acc. Chem. Res.* **35**, 7 (2002). doi:10.1021/ar010110q
- D.C. Metrikin, R. Anand, *Curr. Opin. Ophthalmol.* **5**, 3 (1994). doi:10.1097/00055735-199406000-00005
- S.Z. Razzacki, P.K. Thwar, M. Yang, V.M. Ugaz, M.A. Burns, *Adv. Drug Deliv. Rev.* **56**, 2 (2004)
- R. Ritch, M.B. Shields, T. Krupin, *The Glaucomas* (Mosby, St. Louis, 1989)
- J.T. Santini, M.J. Cima, R. Langer, *Nature* **397**, 6717 (1999)
- D. Smerdon, *Curr. Anaesth. Crit. Care* **11**, 6 (2000). doi:10.1054/cacc.2000.0296
- M.A. Unger, H.P. Chou, T. Thorsen, A. Scherer, S.R. Quake, *Science* **288**, 5463 (2000). doi:10.1126/science.288.5463.113
- J.T. Wilensky, *Curr. Opin. Ophthalmol.* **10**, 2 (1999). doi:10.1097/00055735-199904000-00005
- H.K. Wu, B. Huang, R.N. Zare, *Lab Chip* **5**, 12 (2005). doi:10.1039/b418042a
- B. Ziaie, A. Baldi, M. Lei, Y. Gu, R.A. Siegel, *Adv. Drug Deliv. Rev.* **56**, 2 (2004). doi:10.1016/j.addr.2003.09.001